2021

Design and Development of a Human Building Interaction Laboratory

Sourabh Yadav
Purdue University, United States of America

Parveen Dhillon
Purdue University, United States of America, pdhillon@purdue.edu

Orkan Kurtulus
Purdue University, United States of America

Charles Baxter
Purdue University, United States of America

Davide Ziviani
Purdue University, United States of America

See next page for additional authors

Design and Development of a Human Building Interaction Laboratory

Sourabh D. YADAV[1]*, Parveen DHILLON[1], Orkan KURTULUS[1], Charles BAXTER[1], Davide ZIVIANI[1], Travis HORTON[2], Panagiota KARAVA[2], James E. BRAUN[1],

[1]Ray W. Herrick Laboratories, School of Mechanical Engineering, Purdue University, West Lafayette, IN, USA

[2]Lyles School of Civil Engineering, Purdue University, West Lafayette, IN, USA

yadav35@purdue.edu; pdhillon@purdue.edu; orkan@purdue.edu; cbaxter@purdue.edu; dziviani@purdue.edu; wthorton@purdue.edu; pkarava@purdue.edu; jbraun@purdue.edu

* Corresponding Author

ABSTRACT

A future is envisioned where buildings are assembled on-site from factory manufactured modular elements that integrate the smart technology needed to enable scalable, cost-effective solutions with autonomous, occupant-responsive, healthy, and sustainable features. The use of modular elements would mean that buildings are assembled rather than constructed on-site with better quality control, less material waste, and more predictable schedules. The use of manufactured building elements can enable more cost-effective integration of new sensors, embedded intelligence, networking, adaptive interfaces, renewable energy, energy recovery, comfort delivery, and resiliency technologies, making high-performance buildings more affordable. To explore and evaluate these modular and intelligent comfort delivery concepts and advanced approaches for interaction with occupants, a new human-building interaction laboratory (HBIL) has been designed and is under development. The facility has a modular construction layout with thermally active panels. The interior surface temperature of each panel can be individually controlled using a hydronic system. Such configuration allows us to emulate different climate zones and building type conditions and perform studies such as the effect of different active building surfaces on thermal comfort, localized comfort delivery, and occupant comfort control, among others. Moreover, each panel is reconfigurable to allow investigating different interior surface treatments for different visual and acoustic comfort conditions. In this paper, the overall design approach of the facility is presented. Furthermore, a prototype panel has been constructed to validate the design and assess the dynamic and steady-state thermal performance. Test results for the prototype panel are also presented here with a discussion on their agreement with design phase modeling results.

1. INTRODUCTION

In an envisioned future, modular building elements can interact with occupants to optimize energy usage and provide localized thermal comfort. These human-building interaction concepts could involve smart sensors and voice assistants with advanced control systems and technologies. However, before these innovative building technologies are implemented in the field, they need to be engineered and evaluated, both technology-wise and occupant perception-wise. Radiant heating and cooling (radiant systems) is one of the ways to provide local thermal comfort with modular wall elements and thermo-active surfaces. Rhee & Woo (2015) reviewed the development in radiant heating and cooling systems over the past fifty years and suggested future research areas that would improve radiant heating and cooling technologies. These include designing a system that can provide heating, cooling with multi-zone control, developing practical and straightforward technology to sense surface temperature, optimizing hydronic equipment for radiant systems, and integrating radiant systems with building envelopes. The concept of a human-building interaction laboratory (HBIL) with thermo-active wall panels was conceived to study modular construction, localized thermal comfort delivery, development of radiant heating and cooling systems with multi-zone control, application of intelligent sensors and advanced control approaches, and different novel comfort delivery technologies embedded in

walls such as micro heat pump systems, thermoelectric devices, among others. Figure 1 illustrates the HBIL concept where an occupant inside a space equipped with thermally active panels is communicating with an integrated smart voice assistant for control. The occupant provides a command stating that he/she is feeling hot. In turn, the voice assistant sends a command to the controller to provide localized space cooling around the occupant with thermo-active panels to provide the desired thermal environment.

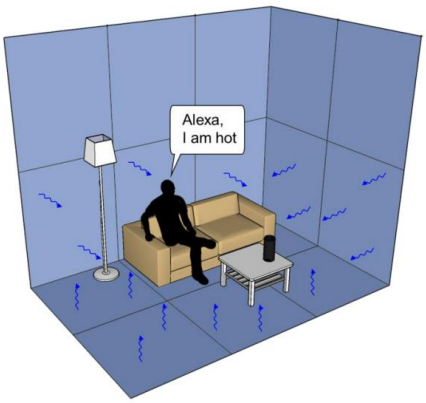

Figure 1. Modular comfort delivery with voice control

The HBIL facility is a 6.1m × 3.65m × 3.04m (20' × 12' × 10') (length x width x height) reconfigurable test-space to facilitate laboratory research for residential and commercial building systems. It will be able to emulate conditions for one or two exterior walls with a glazing area on one wall to enable a realistic representation of a house or a perimeter office space. It will also allow the evaluation of localized thermal comfort using thermo-active surfaces and generate initial data on occupant interactions with modular comfort delivery systems using novel audio and visual interfaces. The main design features include modular construction, reconfigurable wall and interior surface finishes, thermally active wall panel elements, variable/localized thermal comfort delivery, reconfigurable lighting/visual comfort, and reconfigurable acoustic comfort.

The facility is designed to have the capability to individually control the interior surface temperature of each panel, thus allowing studies of the effect of surface temperature on thermal comfort, localized occupant comfort control, and so on. In addition, the facility will also have air comfort delivery capabilities. For this, slot diffusers are embedded in some of the ceiling panels, which will be connected to a main supply air duct from an air-handling unit (AHU). Figure 2 shows the exploded view of the final design of the thermo-active wall panel, and Figure 3 shows the isometric view of the overall facility design.

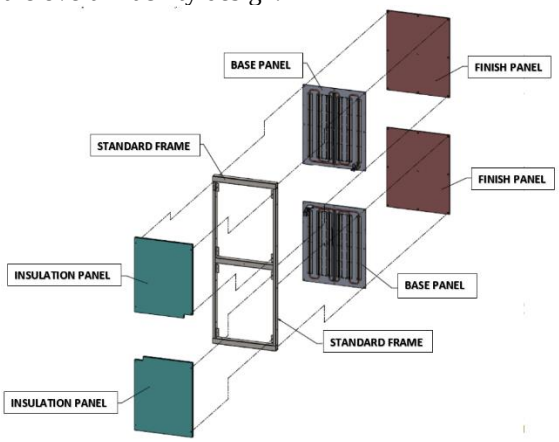

Figure 2. Panel exploded view

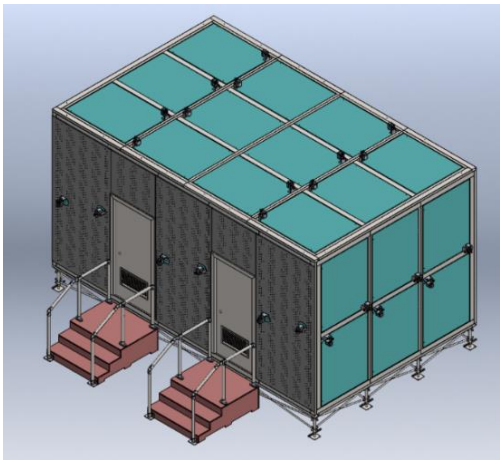

Figure 3. HBIL facility isometric view

This paper presents the HBIL facility design approach with detailed steps leading to the final design configuration. The design and testing of a prototype wall panel to study and validate the design is also presented. A 1-D transient numerical model of the panel and its validation based on test results are also presented in this paper.

2. FACILITY DESIGN APPROACH

To help in determining the range of internal surface temperatures required in the test facility, the DOE reference (Deru et al., 2011) small-office building model was used to simulate energy flows for Chicago. The purpose was to determine typical ranges for interior wall surface temperatures for both winter and summer conditions. Based on the simulation results and typical surface temperatures for floor/ceiling radiant heating and cooling systems, a surface temperature range of 15.5-26.7°C (60°F−80°F) was selected for the scope of research to be performed in this facility.

2.1 Load Estimation

To select an approach, and size equipment for controlling the surface temperature over the range of interest, the first step was to determine facility heating and cooling loads based on heat loss/gain estimates from interior surfaces for the most extreme temperature conditions. Thus, convective and radiative heat gains/losses were estimated for the room dimensions (surface area (A) of walls, floor, and ceiling), interior surface temperature ($T_{surface}$), and indoor air temperature (T_{air}) conditions that are shown in Table 1.

Table 1. Load estimation design parameters

Room Dimension: 20×12×10 ft	Heating Design Temperatures	Cooling Design Temperatures
A_{wall} = 640 ft^2 (59.2 m^2) $A_{floor} = A_{roof}$ = 240 ft^2 (22.3 m^2)	$T_{surface}$ = 80°F (26.7°C) T_{air} = 70°F (21.1°C)	$T_{surface}$ = 60°F (15.5°C) T_{air}= 74°F (23.3°C)

The convective heat transfer from the interior surfaces (walls and floor) was estimated using convective heat transfer correlations from Goldstein & Novoselca (2010) based on the designed comfort delivery system implementation with ceiling diffusers. The radiative heat transfer from the interior surfaces (walls and floor) was estimated using a radiative heat transfer correlation from Bergman et al. (2011) in which the long-wave radiation is linearized with a view factor of unity. Table 2 shows the load estimation results based on heat transfer from interior surfaces (walls and floor) for the heating and cooling case. The heating case represents the minimum heating input required to maintain a positive heat gain to the room from the interior surfaces at the specified conditions. The negative sign in the cooling case conveys that the heat transfer is into the surface from the indoor air.

Table 2. Load estimation for heating and cooling case

Operation Mode	Convection [W]	Radiation (*1) [W]	Total [W]	Heat Flux [W/m^2]
Heating	1592	2592	**4184**	**51**
Cooling	-2229	-3469	**-5698**	**-70**

*1 Radiation heat transfer assuming worst-case scenario for each surface, i.e., the surface in the calculation is at $T_{surface}$ whereas other walls, floor, and roof are at T_{air}, and assuming paint (ϵ=0.96)

2.2 Investigation of Design Approaches for Panel Surface Temperature Control System

Four different system design approaches were investigated to control panel surface temperature for heating and cooling. Each approach was evaluated based on its potential to provide both heating and cooling to satisfy the design conditions, ease of individual panel temperature control, and overall cost. Table 3 summarizes the different design approaches along with their pros and cons. Based on these considerations, a hydronic system that uses chilled and hot water loops with mixing valves was selected for controlling surface temperatures of individual panels. A detailed description of the panel design and performance is presented in Section 3.1.

Table 3. Design approaches for HBIL facility

Design Approach	Description	Remarks
Thermoelectric based system	Thermoelectric modules embedded in the test facility surfaces for both heating and cooling.	Has the capability to provide both heating and cooling and can meet the required heat flux. However, this system would have required many modules and control hardware due to the small size of each module, thereby leading to very high total cost.

Cold air and heating element based system	Cold air through ducts between the interior surface. Exterior insulation layer for cooling and resistive heating element for heating.	An airflow with a velocity of 1 m/s would not be sufficient to maintain the interior surface temperature at the lowest target setpoint. Higher air velocities could result in noise issues.
Chilled water and heating element based system	Chilled water through tube-heat spreader attached to the interior surface for cooling, resistive heating element for heating.	With this design configuration, the lower thermal resistance between the heating element and the chilled water loop compared to the thermal resistance between the heating element and the indoor air could lead to control issues and very large cooling requirements when the system is operating in the transition between cooling and heating mode.
Chilled and hot water-based system	Cold and hot water loop with a 3-way mixing valve to control the supply water temperature and subsequently control the panel surface temperature.	This system suits the design requirements for surface temperature target range and with a reasonable control approach without any issues mentioned above for other design approaches.

For the chosen system configuration, the panel interior surface temperatures are controlled based on mixing chilled and hot water for the desired target temperature. The idea is to have two parallel chilled and hot water loops and utilize a 3-way mixing valve to change the water inlet temperature to each panel to maintain the desired interior surface temperature. The water flow rate in each panel is kept constant to reduce the overall system cost and control complexity.

Preliminary steady-state simulations were performed in EES (Engineering Equation Solver) (Klein, 2021) using a finite volume model of the panel described in Section 3.2 to determine a water flow rate to achieve an acceptably uniform temperature distribution over the panel surface. In the simulation, the inside air temperature (T_{ID}) was assumed to be 21.11°C (70°F), and the outside air temperature was 23.33°C (74°F) (as the facility will be located in an indoor environment). Figure 4 shows the steady-state temperature distribution across the panel height for a cooling case, with a water inlet temperature of 12.77°C (55°F) and a flow rate of 0.95 GPM. Figure 5 shows simulation results with the same flow rate for a heating case, with a water inlet temperature of 29.44°C (85°F). It can be seen from both the plots that this water flow rate results in a temperature change in water (black line) across the panel height of around 0.6°C (1.2°F) and a temperature difference along the panel surface (green line) of around 0.7°C (1.4°F). These are within acceptable limits. Based on the analysis results and 3-way mixing valve selection constraints, the water flow rate for each cooling circuit of a panel was specified to be 1 GPM.

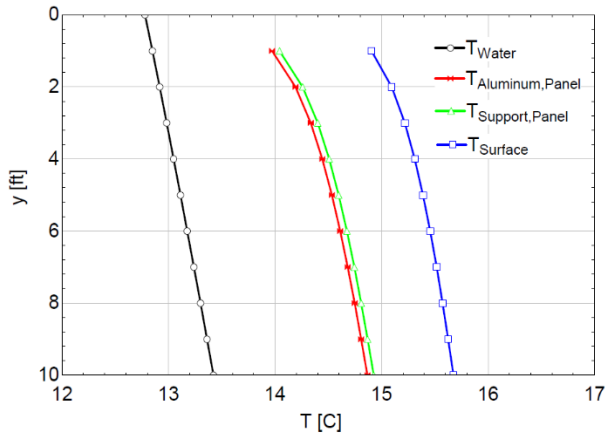

Figure 4. Panel steady-state simulation results for cooling

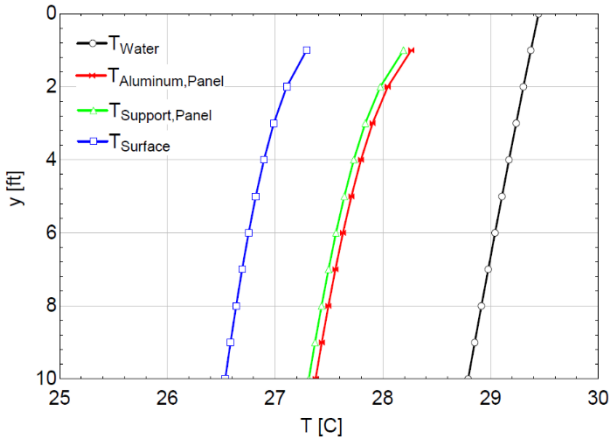

Figure 5. Panel steady-state simulation results for heating

The facility will be composed of 52 modular 1.22m × 1.52m (4'×5') (width × height) wall, ceiling, and floor panels attached to an overall frame. A four-pipe hydronic distribution system will provide hot and cold water to pairs of panels that are arranged in a series flow arrangement as depicted in Figure 6. The hot and cold water will be mixed using a 3-way valve to allow individual control of a temperature at the interior surface of each panel pair. There will also be a diverting valve at the outlet of each panel pair that will divide the mixed water into hot and cold water return loops in the same proportion as the mixing valve in order to maintain balanced flows. The hydronic system will continuously circulate cooling and heating water in the two separate loops to each 3-way mixing valve. A temperature sensor will be embedded in an appropriate location at the interior surface treatment of each 4'×5' panel and used to provide feedback control of local comfort conditions within the interior space. A water-to-water heat pump will provide heat transfer between chilled and hot water tanks that will be coupled to the chilled and hot water loops. In addition, there will be a resistance heating element in the hot water tank and an auxiliary hot water fan coil unit for heat rejection that will be used, when necessary, for load balancing. Pressure-regulating valves will be employed in both hot and cold water loops to maintain the required head pressure. The 3-way valves will be adjusted using feedback control based on surface temperature setpoints that can vary locally within the indoor space. Humidity control and ventilation requirements will be satisfied by dedicated air diffusers.

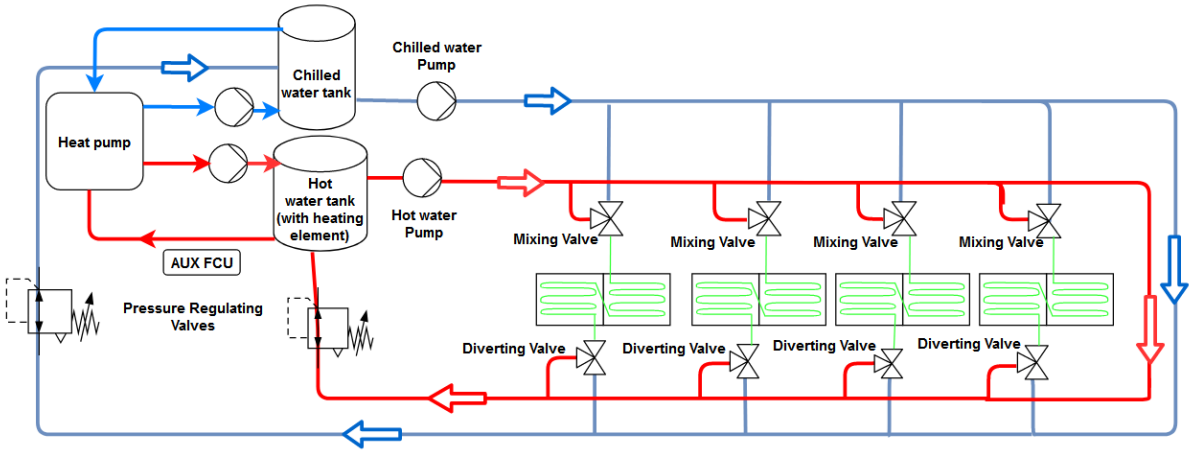

Figure 6. HBIL facility hydronic system

3. PROTOTYPE PANEL DESIGN, TESTING, AND NUMERICAL MODEL VALIDATION

A prototype panel was constructed to validate the design and assess the steady-state and dynamic thermal performance of the panel and it is shown in Figure 7. As mentioned before, the design goal for the panel was to provide uniform surface temperature from 15.5°C (60°F) to 26.7°C (80°F). Additional transient response criteria were established, so that panel surface temperature would be able to change from minimum to maximum design value in less than 50 minutes. A numerical model was developed for the panel that is described in this section, along with steady-state and transient response validation results. This numerical model will be useful as a tool to design alternative wall panels with different surface treatments in the future.

A test setup for a prototype panel testing was designed and constructed, as shown in Figure 8. Twelve thermocouple sensors were attached to measure the surface temperature, as shown in the front view. One thermocouple sensor was attached to the back panel to measure aluminum backplate temperature, as shown in the 'rear view' of Figure 8. Hot, cold, and mixed water temperatures were measured using in-line thermocouples inserted in the water stream. Hot and cold water bypass valves were used to maintain the constant head pressure on the hot and cold loop. Head pressures of hot, cold, and mixed water were also measured. Furthermore, a differential pressure sensor is installed between the inlet and outlet of the panel to estimate the pressure drop across the panel.

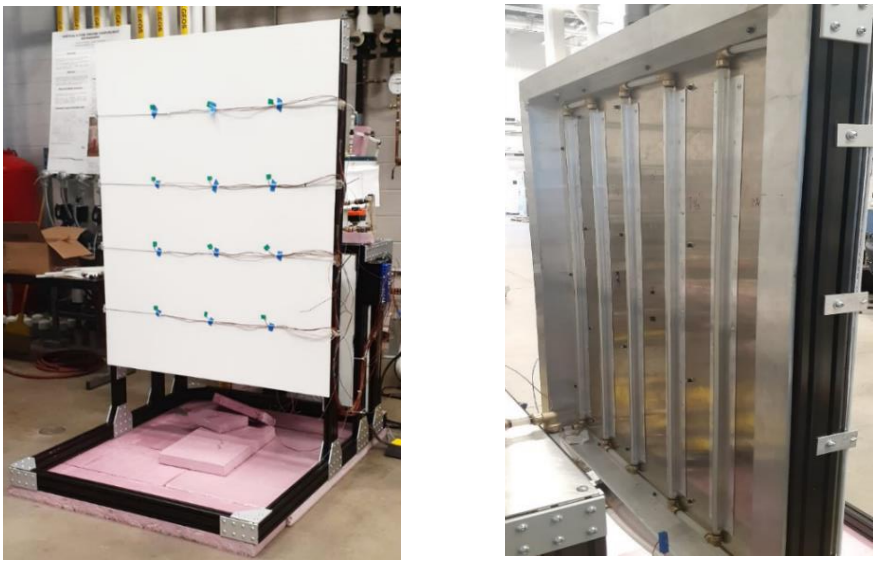

Figure 7. Prototype panel test setup

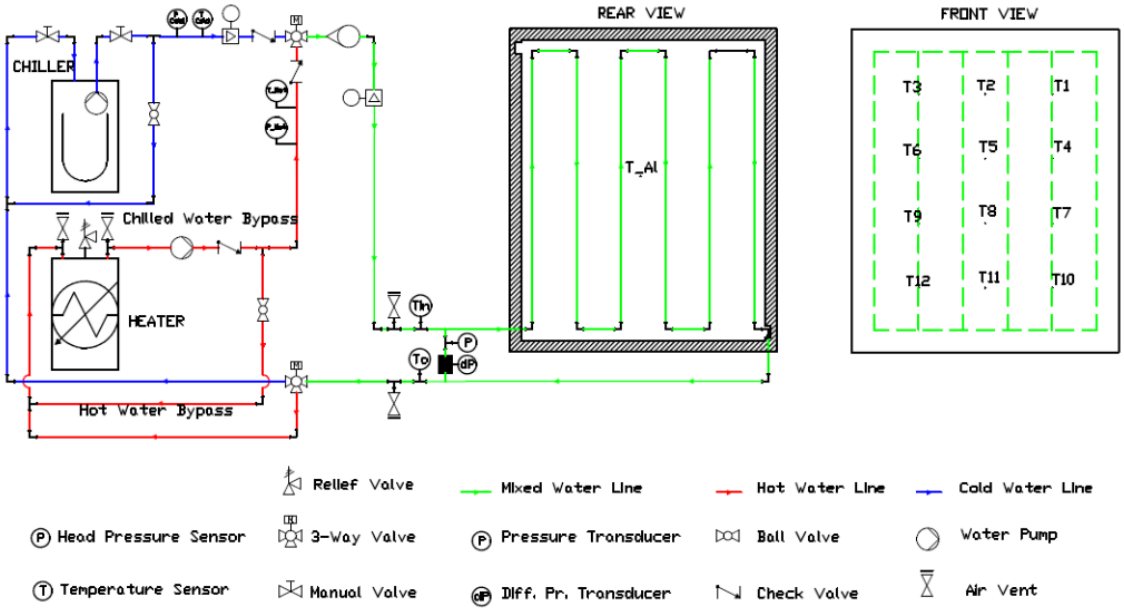

Figure 8. Prototype panel test setup schematic drawing

A temperature stratification was observed in the room air temperature from the ground level to 7 feet height. The air temperature at 1 foot above the floor was around 1°C lower than the temperature at a level of 7 feet above the floor level. Also, because all the panel layers were installed inside an aluminum frame, it was assumed that there would be heat transfer occurring through the edges of the panel, thereby resulting in sightly different surface temperature readings as compared to the central part. Keeping these factors in mind, the design goal was to have the surface temperature distribution across the twelve thermocouples to be within 1°C to 1.5°C. Different piping configurations were tested to achieve uniform surface temperature distribution across the panel surface along the same horizontal plane of a specific elevation from the floor. A series flow configuration was finalized because the parallel piping configurations showed non-uniform flow across different parallel passes, which led to a non-uniform surface temperature distribution. Six heat spreaders are used for the six straight sections of copper tubing. They have a semi-circular cavity slot to hold the copper tubes on one side and have a flat surface on the other side attached to the flat aluminum backplate surface. Based on experimental investigation, C-type heat spreaders showed better heat transfer capability than the U-type heat spreader. Figure 9 shows C-type and U-type heat spreaders.

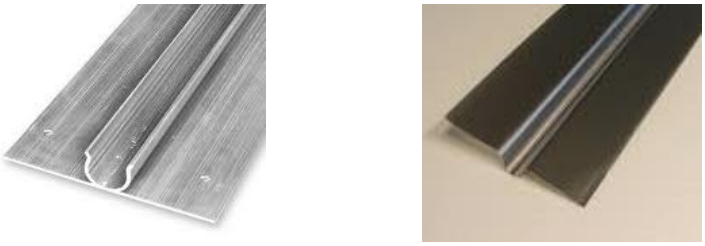

C-type heat spreader U-type heat spreader

Figure 9: Heat Spreaders

3.1 Panel Performance Limit Assessment

Limits on the panel thermal performance were assessed for heating and cooling mode by evaluating the maximum and minimum surface temperature the panel can achieve with the given chiller and heater capacities for typical indoor conditions. The temperature on the panel surface was measured at twelve locations, as shown in the 'front view' of Figure 8. In a performance assessment test, the heating mode was initiated at first, and hot water at 45°C was circulated through the hydronic circuit at the panel back until the surface temperature reached a steady-state. After a 10-minute steady-state measurement, the system was switched to cooling mode, and chilled water at 4.5°C circulated through the panel until a steady-state was reached.

Figure 10 shows test results with PEX tubing in the hydronic circuit at the back of the panel. The design goal for the surface temperature in heating and cooling was achieved; however, the transient response was slow. It took around 90 minutes to reach the minimum surface temperature from the maximum, which did not meet the transient design goal. To improve the transient response of the panel, PEX tubes were replaced with better-conducting copper tubes. This modification resulted in a faster dynamic response in heating as well as in cooling mode, as shown in Figure 11. The time required to reach maximum heating or minimum cooling steady-state temperature was reduced by 40% compared to the PEX tubing case. In addition to the quicker response, there was around a 2ºC rise in heating and a 1.5°C drop in cooling steady-state panel surface temperature compared to the test with PEX tubing. Further, the effect of rear insulation on the panel surface temperatures was also studied, as shown in Figure 11. Without rear insulation, the surface temperature dropped around 1°C due to heat losses from the panel back surface.

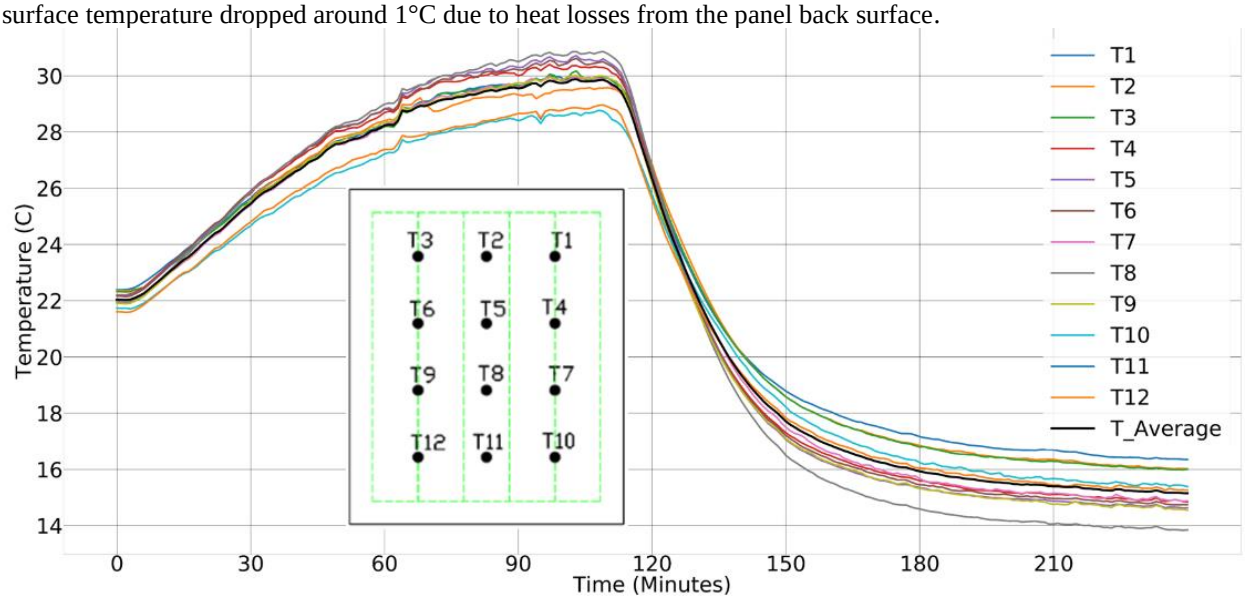

Figure 10. PEX tubing performance limit test results

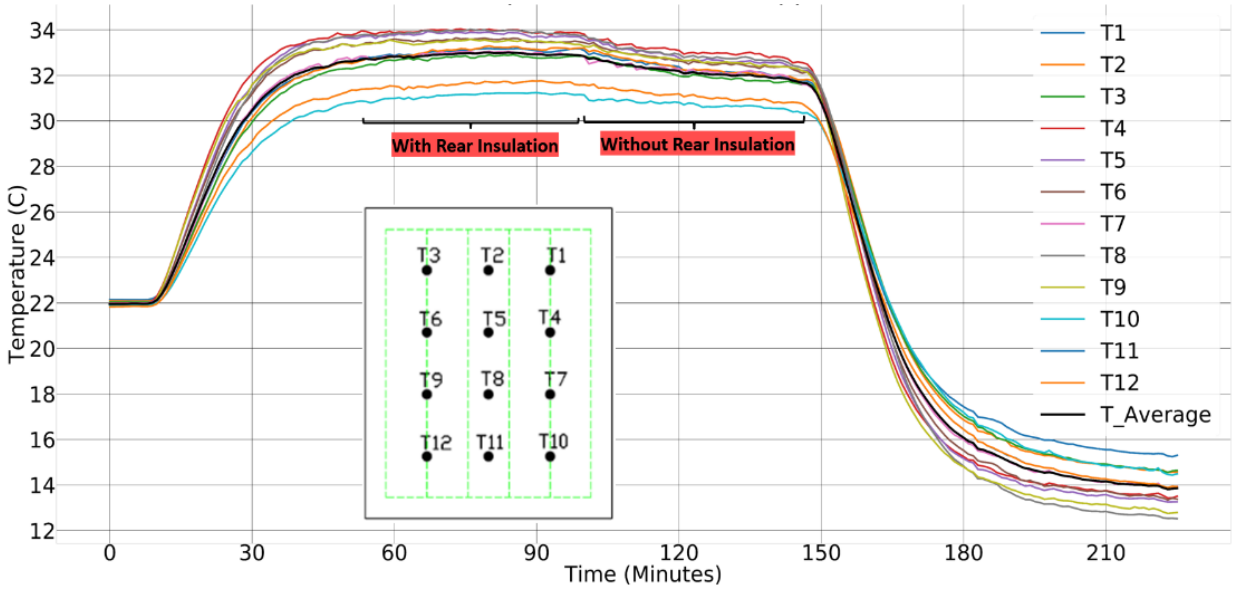

Figure 11. Copper tubing performance limit test results

Figure 12 and Figure 13 are panel surface thermal images during steady-state heating and cooling conditions with copper tubing, respectively. A significant heat loss was observed from the panel edges. Consequently, the region with the lowest temperature value was in the center of the panel. This temperature distribution aligns with the thermocouple readings plotted in Figure 11. It can also be observed that the temperature measured by thermocouples closer to the floor (T12, T11) was lower than the rest of the thermocouples, which aligns with the indoor air temperature stratification explained above. It should be noted that panel edge losses should be dramatically reduced when the panels are installed within the facility if adjacent panels are operating at similar conditions. It should also be noted that these experiments were extremely useful in finalizing the prototype panel design and validating the model, as described in the next section.

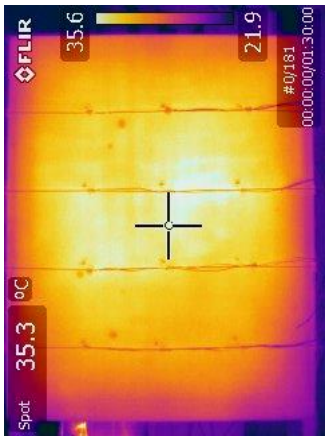

Figure 12. Heating steady-state thermal image

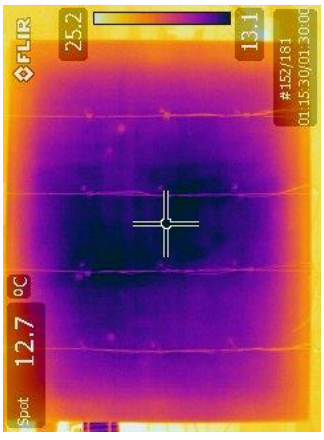

Figure 13. Cooling steady-state thermal image

3.2 Validation of Prototype Panel Heat Transfer Model Using Experimental Results

The prototype wall panel is essentially a composite wall with copper tubes embedded in heat spreaders on the backside and a gypsum layer on the front side. A 1-D transient thermal network model for this prototype wall panel was developed in EES (Klein, 2021). The critical inputs for the model are mixed water inlet temperature, outdoor temperature, and indoor air temperature values. The model calculates values of panel surface temperature, water outlet temperature, and aluminum backplate temperature. In addition, the heat transfer that occurs from water to the indoor air ($\dot{Q}_{front}$) and the heat lost to the outdoor air ($\dot{Q}_{loss}$) are computed. The model uses 'bond conductance' to account

for the thermal resistance for heat transfer between water and the heat spreader. The model was tuned by varying the values of bond conductance, capacitances, and thermal and contact resistances. Figure 14 shows the thermal network diagram for the model with different layers of the prototype wall panel.

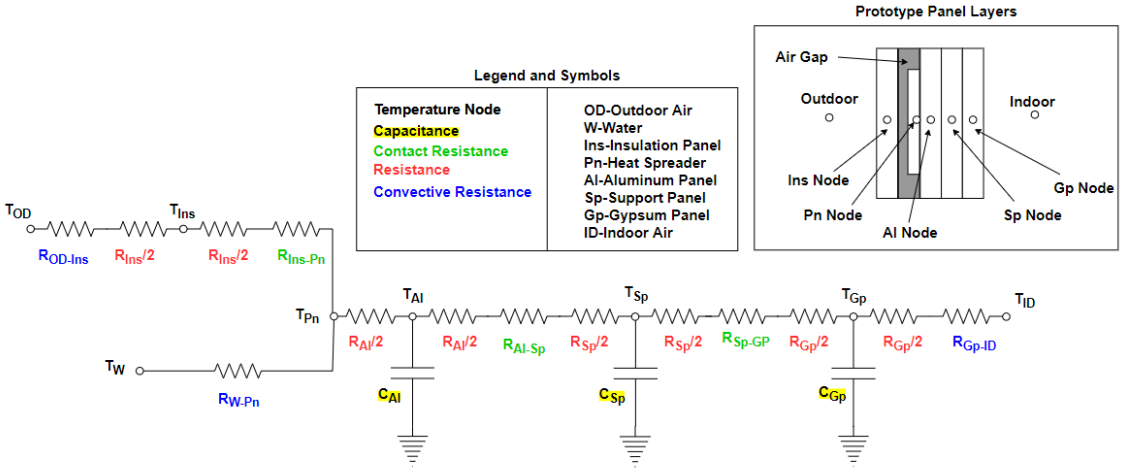

Figure 14: Thermal network model for prototype panel

The thermal circuit in Figure 14 leads to the following equations (equations 1-4) that represent the heat transfer rates. To model heat transfer from copper tubes to the heat spreader panel, equation 5 is used, which is analogous to a solar flat plate collector scheme (Kalogirou, 2009). The heat transfer coefficient between the water and tube inner surface (h_{fi}) is evaluated using an inbuilt EES function for internal pipe flow from Nellis and Klien (2009). Convective and long-wave radiative heat transfers to or from the panel surface are assumed to occur in parallel with exchange occurring with a common indoor condition. The long-wave radiation is linearized with a view factor of unity (Bergman et al., 2011) to the surrounding surfaces (equation 6). In contrast, a natural convection correlation from Nellis and Klein (2009) for a vertical wall (also an EES built-in function) is employed.

$$\dot{Q}_{in} = \dot{Q}_{front} + \dot{Q}_{loss} \tag{1}$$

$$\dot{Q}_{in} = (T_{W\,in} - T_{Pn})/R_{W-Pn} \tag{2}$$

$$\dot{Q}_{loss} = (T_{Pn} - T_{OD})/R_{Ins-Al} \tag{3}$$

$$\dot{Q}_{front} = (T_{Pn} - T_{Al})/(R_{Panel} + R_{Gp-ID}) \tag{4}$$

$$q'_u = \frac{(T_b - T_f)}{(1/C_b) + (1/\pi D_i h_{fi})} = q'_{fin} + q'_{tube} \tag{5}$$

$$h_r = \varepsilon_{gp} \times \sigma \times \left(T^2_{Surface} + T^2_{ID}\right) \times (T_{Surface} + T_{ID}) \tag{6}$$

where $\dot{Q}_{in}$ is the heat transfer rate from the water inside the tubes to the heat spreader node, $\dot{Q}_{front}$ is the heat transfer rate from the heat spreader node to indoor air through interior surface treatment and $\dot{Q}_{loss}$ is the heat transfer rate occurring from the heat spreader node to outdoor air through insulation panel. The thermal capacitances of the heat spreader (due to its small size and mass) and insulation panel (due to its low mass density) are neglected because they were found not to significantly contribute to the transient behavior of the prototype wall panel. Using the heat transfer rate ($\dot{Q}_{front}$), an energy balance was set up to calculate a time-dependent temperature gradient (dT_{Al}/dt) equation 7. This was integrated numerically over the total duration of the test (Et) to calculate aluminum node temperature (T_{Al}) (equation 8). A similar set of energy balance and integration equations were set up between the aluminum and support panel nodes and between the support and gypsum panel nodes to calculate panel surface temperature. The equation system is closed by an energy balance (equation 9) between the total heat transfer rate entering the system and energy gained or lost through interaction with the cooling or heating water, respectively.

$$\dot{Q}_{front} = \{Cap_{Al} \times (dT_{Al}/dt)\} + \frac{(T_{Al} - T_{Sp})}{(R_{Al}/2 + R_{Sp}/2 + R_{Al,Sp}/2)} \quad (7)$$

$$T_{Al} = T_{ID} \times \int_0^{Et} (dT_{Al}/dt)\ dtime \quad (8)$$

$$\dot{Q}_{in} = \dot{m}_w \times Cp_w \times (T_{w,out} - T_{w,in}) \quad (9)$$

The key outputs of the model are surface temperatures and aluminum backplate temperatures obtained for each time step (every minute). Figure 15 shows the panel surface temperature results from the tuned model (T_{Model}) and experiments (T_{Expt}). It can be seen that model results are within 0.5 °C of the experimental results throughout the test interval. Similarly, Figure 16 shows the aluminum backplate temperature results ($T_{Al,Back,Model}$) overlaid on experimental results ($T_{Al,Back,Expt}$). In this case, the differences in the model and experimental values are slightly higher, about 1°C, especially at steady-state. This is because the sensor measuring the aluminum backplate temperature was covered using insulation tape, thereby blocking the convective and radiative heat transfer with the air. This resulted in lower values for steady-state cooling and higher values steady-state heating cases. On the contrary, the temperature sensors on the panel surface had a transparent thin thermal tape allowing relatively more convective and radiation heat exchange with the indoor air. Additional validation tests were performed on the prototype at different operating conditions with similar results.

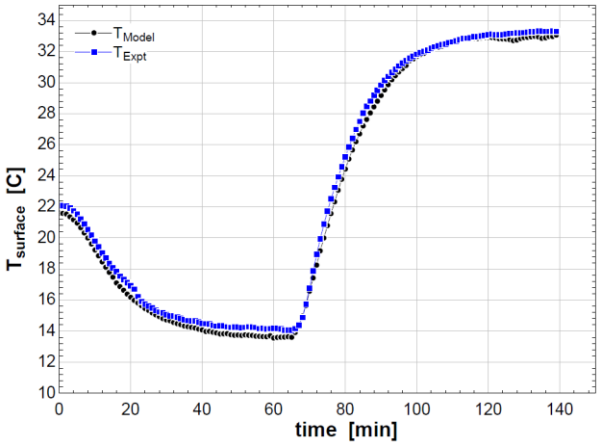

Figure 15. Comparisons of the model and experimental results (Panel surface temperature)

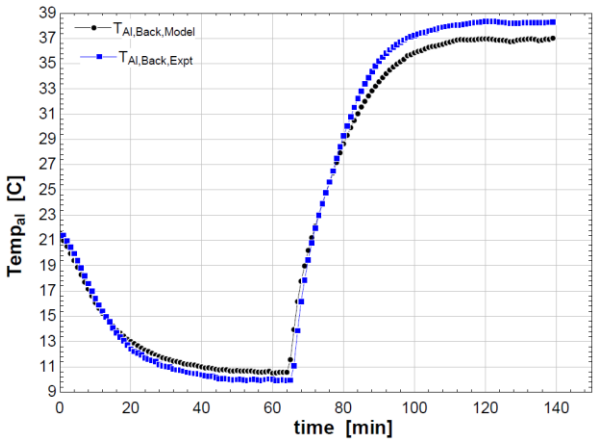

Figure 16. Comparison of the model and experimental results (Aluminum backplate temperature)

4. CONCLUSIONS

This paper presented an overview and design of a human-building interaction laboratory (HBIL) that will enable evaluation of next-generation concepts for comfort delivery and building interaction. Furthermore, a prototype thermally active panel for the facility was presented along with the assessment of its transient and steady-state thermal performance. The panel is capable of generating a wide range of interior surface temperatures that could be locally controlled to provide local heating or heating within the facility. Modeling results for the panel agree well with measurements, such that the model could be used in the future to develop alternative thermally active panels for installation in this modular facility.

The future steps involve the assembly of the HBIL facility, installation and commissioning of the facility's hydronic system, design, commissioning of control architecture, and voice interaction. Once fully commissioned, the facility will be used to emulate different climate zones and/or study localized thermal comfort delivery with human test subjects.

NOMENCLATURE

Symbols		Subscripts	
T:	Temperature	Pn:	Heat Spreader Panel
R:	Thermal Resistance	Al:	Aluminum Back Panel
R_C:	Thermal Contact Resistance	Sp:	Support Panel
$\dot{Q}_{loss}$:	Heat transfer rate from *Al* to *OD* through *Ins* (W)	Gp:	Gypsum Panel
$\dot{Q}_{in}$:	Heat transfer rate from *W* to *Al* through *Pn* (W)	Ins:	Insulation Panel
$\dot{Q}_{front}$:	Heat transfer rate from *Al* to the *Surface* (W)	W:	Water
D_i:	Tube Internal Diameter (m)	ID:	Indoor Air
q'_u:	Heat rate per unit length of the tube (W/m)	OD:	Outdoor Air
C_b:	Bond Conductance (W/m-K)	$Surface$:	Panel Surface
h_{fi}:	*W*-Tube inside wall heat transfer coefficient (W/m^2-K)		
h_c:	*Surface-ID* convective heat transfer coefficient (W/m^{2}K)		
h_r:	*Surface-ID* radiative heat transfer coefficient (W/m^{2}K)		
ΔT:	$T_{surface}$- T_{ID}		
ε_{gp}:	Emissivity for gypsum surface		
σ:	Stefan-Boltzmann constant (W/m^{2}K^4)		
T_b:	*Al* Temperature (K)		
T_f:	Water Inlet Temperature (K)		

REFERENCES

Bergman, T., Lavine, A., Incropera, F., & Dewitt, D. (2011). Radiation. In *Fundamentals of Heat and Mass Transfer* (7th ed., pp. 8–10). John Wiley & Sons.

Deru, M., Field, K., Studer, D., Benne, K., Griffith, B., Torcellini, P., Liu, B., Halverson, M., Winiarski, D., Rosenberg, M., Yazdanian, M., Huang, J., & Crawley, D. (2011). U.S. Department of Energy commercial reference building models of the national building stock. *Publications (E), February 2011*, 1–118. http://digitalscholarship.unlv.edu/renew_pubs/44

Goldstein, K., & Novoselca, A. (2010). Convective Heat Transfer in Rooms with Ceiling Slot Diffusers. *HVAC&R RESEARCH*, *16*(5), 629–655. https://doi.org/http://dx.doi.org/10.1080/10789669.2010.10390925

Kalogirou, S. (2009). *Solar Energy Engineering* (an O. M. C. Safari (Ed.); 1st edition) [Book].

Klein, S. A. (2021). *EES-Engineering Equation Solver* (Academic Professional V-10.834-3D [2020-05-27]). www.fChartSoftware.com

Nellis, G. (2009). *Heat transfer* (Sanford A. Klein (Ed.)) [Book]. Cambridge University Press.

Rhee, K., & Woo, K. (2015). A 50 year review of basic and applied research in radiant heating and cooling systems for the built environment. *Building and Environment*, *91*, 166–190. https://doi.org/10.1016/j.buildenv.2015.03.040

ACKNOWLEDGEMENTS

Development of the HBIL was funded, in part, by the Center for High Performance Buildings at Purdue. The design and manufacturing of all the panels and base structure and its installation are being carried out by Bridgewater Studious. Their support and work are greatly appreciated. The essential equipment of the facility's hydronic system have been donated by WaterFurnace (Heat Pumps and Water tanks), Belimo (3-way mixing valves), and Johnson Controls (Auxiliary Fan Coil Unit). The HBIL team is very grateful for their interest in this project and the equipment donations. We also acknowledge Feng Wu, our fellow research student contributing to the voice-control system design and its integration with the HBIL facility and future HBIL testing. Lastly, the HBIL team is grateful to the Herrick shop staff for their technical support and guidance.